

# The *ERBB2* c.1795C>T, p.Arg599Cys variant is associated with left ventricular outflow tract obstruction defects in humans

Minna Ampuja,<sup>1</sup> Sabina Ericsson,<sup>1</sup> Ilkka Paatero,<sup>2</sup> Iftekhar Chowdhury,<sup>3</sup> Jenna Villman,<sup>2</sup> Martin Broberg,<sup>1,4</sup> Amanda Ramste,<sup>1</sup> Diego Balboa,<sup>1</sup> Tiina Ojala,<sup>5</sup> Jessica X. Chong,<sup>6</sup> Michael J. Bamshad,<sup>6</sup> James R. Priest,<sup>7,8</sup> Markku Varjosalo,<sup>3</sup> Riikka Kivelä,<sup>1,9,10,12</sup> and Emmi Helle<sup>1,5,11,12,13,\*</sup>

## Summary

Non-syndromic congenital heart defects (CHDs) are occasionally familial and left ventricular outflow tract obstruction (LVOTO) defects are among the subtypes with the highest heritability. The aim of this study was to evaluate the pathogenicity of a heterozygous *ERBB2* variant c.1795C>T, p.Arg599Cys identified in three families with LVOTO defects. Variant detection was done with exome sequencing. Western blotting, digital PCR, mass spectrometry (MS), MS microscopy, and flow cytometry were used to study the function of the *ERBB2* variant c.1795C>T. Cardiac structure and function were studied in zebrafish embryos expressing human *ERBB2* wild type or c.1795C>T. Proband-derived human induced pluripotent stem cell cardiomyocytes (hiPS-CMs) and endothelial cells (hiPS-ECs) were used for transcriptomic analyses. While phosphorylation of the *ERBB2* p.Arg599Cys receptor was not altered, the variant affected dramatically the binding partners of the protein, indicating mislocalization of the mutant *ERBB2* from plasma membrane to endoplasmic reticulum. Expression of human *ERBB2* p.Arg599Cys in zebrafish embryos resulted in cardiomyocyte hypertrophy, increased cardiac wall thickness, and impaired fractional shortening. Transcriptomic analyses of hiPS-ECs and hiPS-CMs from an individual with the c.1795C>T variant showed aberrant expression of genes related to cardiovascular system development and abnormal response to oxidative stress in both cell types. In conclusion, the heterozygous variant *ERBB2* c.1795C>T, p.Arg599Cys leads to abnormal cellular localization of the *ERBB2* receptor and induces structural changes and dysfunction in the zebrafish embryo heart. This evidence expands previous findings from animal studies to humans and suggests variants in *ERBB2* may be associated with CHD.

## Introduction

Left ventricular outflow tract obstruction (LVOTO) is a subgroup of congenital heart defects (CHDs) affecting the left side of the heart—the mitral valve, the left ventricle, the aortic valve, and the aorta. The severity of LVOTO defects range from the often initially asymptomatic bicuspid aortic valve (BAV, MIM: 109730) to complex defects, such as hypoplastic left heart syndrome (HLHS, MIM: 241550), representing one of the most severe forms of CHD. In HLHS, mitral and aortic stenosis or atresia combined with left ventricular hypoplasia result in the left side of the heart incapable of adequately supporting the systemic circulation. This necessitates palliative procedures, ultimately leading to the establishment of single ventricle physiology.

Non-syndromic CHDs are often hereditary, and LVOTO defects are among the subtypes with the highest heredit-

ability—they have been shown to be associated with a 20% incidence of CHD in the first-degree relatives.<sup>1,2</sup> Around 5%–15% non-syndromic CHDs are estimated to be monogenic, and it has been suggested that the majority of CHDs are oligogenic with two or more predisposing genetic variants contributing,<sup>3,4</sup> or multifactorial, occurring due to a combination of genetic and environmental risks.<sup>5–8</sup> Indeed, genetic susceptibility in the form of rare risk alleles with modest effect sizes have been observed in genome wide association studies (GWAS) for LVOTO<sup>9,10</sup> as well as for other CHDs.<sup>9,11,12</sup> Out of environmental risks, maternal diabetes, obesity, advanced maternal age, maternal hypertension, maternal medications, and certain viral infections during early pregnancy are the most well documented.<sup>5,13–18</sup>

Identifying genes associated with non-syndromic CHDs and LVOTO defects even in familial cases is complicated by their reduced penetrance and variable expressivity.<sup>19,20</sup>

<sup>1</sup>Stem Cells and Metabolism Research Program, Faculty of Medicine, University of Helsinki, Helsinki, Finland; <sup>2</sup>Turku Bioscience Centre, University of Turku and Åbo Akademi University, Turku, Finland; <sup>3</sup>Institute of Biotechnology, HiLIFE Helsinki Institute of Life Science, University of Helsinki, Helsinki, Finland; <sup>4</sup>Institute for Molecular Medicine Finland, Helsinki, Finland; <sup>5</sup>Children's Hospital, Paediatric Research Centre, University of Helsinki and Helsinki University Hospital, Helsinki, Finland; <sup>6</sup>Division of Genetic Medicine, Department of Pediatrics, University of Washington, Seattle, WA, USA; <sup>7</sup>Tenaya Therapeutics, 171 Oyster Point Boulevard Suite 500, South San Francisco, CA, USA; <sup>8</sup>Department of Pediatrics, Stanford University School of Medicine, Stanford, CA, USA; <sup>9</sup>Wihuri Research Institute, Helsinki, Finland; <sup>10</sup>Faculty of Sport and Health Sciences, University of Jyväskylä, Jyväskylä, Finland; <sup>11</sup>Population Health Unit, Finnish Institute for Health and Welfare, Helsinki, Finland

<sup>12</sup>These authors contributed equally

<sup>13</sup>Lead contact

\*Correspondence: [emmi.helle@helsinki.fi](mailto:emmi.helle@helsinki.fi)

<https://doi.org/10.1016/j.xhgg.2025.100446>.

© 2025 The Authors. Published by Elsevier Inc. on behalf of American Society of Human Genetics.

This is an open access article under the CC BY-NC-ND license (<http://creativecommons.org/licenses/by-nc-nd/4.0/>).



While monogenic forms with autosomal dominant inheritance due for example, to truncating variants in *NOTCH1* (MIM: 190198) have been identified as causal in some LVOTO families with multiple affected members,<sup>21–24</sup> most familial cases remain without a genetic diagnosis. As the yield of genetic testing in isolated CHD is currently low, it is not generally recommended unless there is suspicion of an underlying genetic syndrome.<sup>25,26</sup> An exception to this for left-sided lesions is supravalvular aortic stenosis (SVAS, MIM: 185500), where causal *ELN* variants are occasionally identified.<sup>25</sup>

CHDs are heterogeneous, with each gene accounting for a small number of monogenic causes. Therefore, establishing clear gene-disease relationships is essential for improving the diagnostic yield in CHD. In addition, it may aid to unravel the complex molecular mechanisms of cardiac development and the cellular-level events leading to CHD.<sup>9,10</sup> The relatively genetically homogeneous Finnish population provides an excellent opportunity to identify disease-related variants compared with more heterogeneous populations<sup>27</sup>—especially as there are regional differences in the prevalence of certain CHD subtypes within Finland.<sup>28</sup>

To gain further insight into the genetic etiology of LVOTO and human cardiac development, we conducted exome sequencing in Finnish LVOTO subjects and families with multiple affected members to identify new LVOTO-associated loci. We identified an ultra-rare variant in *ERBB2* (MIM: 164870) that segregated with disease in three unrelated families. *ERBB2* is a member of the epidermal growth factor (EGF) receptor family of receptor tyrosine kinases. *ERBB2* binds to other EGF receptor family members forming heterodimers and signals through Akt, MAPK, and other pathways. *ERBB2* is a known oncogene, but it has also been shown to be essential for heart development in animal models.<sup>29–33</sup> However, its role in the human heart development has not been demonstrated.

## Materials and methods

Expanded materials and methods section is provided in the [supplemental information](#).

### Responsible science

This study has been designed according to The Helsinki Declaration and the Conventions of the Council of Europe on human rights. The study protocols have been approved by the Ethical Committee of Helsinki University Hospital District. Written informed consent has been obtained from all study participants over 6 years of age and from their parents/guardians if the participants are minors. Analyses of zebrafish embryos were carried out under the licenses GTLK/004/E/2016, ESAVI/31414/2020, and ESAVI/44584/2023 (granted by Project Authorization Board of Regional State Administrative Agency for Southern Finland) according to the regulations of the Finnish Act on Animal Experimentation (62/2006). The study was carried out in compliance

with the ARRIVE guidelines and the Directive 2010/63/EU of the European Parliament on the protection of animals used for scientific purposes. The research in this study was performed at University of Helsinki (Finland), University of Turku (Finland), Stanford University (United States), and University of Washington (United States).

### Study cohort and exome sequencing

We recruited a study cohort of 137 pediatric study subjects (age 0–15 years) who were followed up for left ventricular outflow tract obstruction (LVOTO) defects from Helsinki University Children’s Hospital (Table S1). Study subjects with a known or suspected syndrome or study subjects with extracardiac congenital malformations were not included. As our institution does not order genetic testing for isolated CHD, unless syndromic etiology is suspected, none of the included study subjects had undergone previous clinical genetic testing. In addition to the probands, parents were recruited for exome sequencing when available, and in the case of known family history, also other available family members were recruited. Of the 137 study subjects, 79 were singletons, 50 were trios, and eight were families with multiple affected members (total number of sequenced subjects was 274). Study subject recruitment and data collection were done between 2014 and 2023. Exome sequencing was performed by the University of Washington Center for Mendelian Genomics Seattle, USA, and Blueprint Genetics Ltd. All persons sequenced were of self-reported Finnish ancestry.

### Variant calling

After filtering out duplicates and outliers based on genome quality, we used 275 hg38 aligned BAM files from both Blueprint Genetics (BPG, 173 exomes) and University of Washington (UW-CMG, 102 exomes) for variant calling using FreeBayes v1.3.1.<sup>34</sup> We used the following settings for freebayes: `–min-mapping-quality 20 –min-base-quality 20 –min-alternate-count 20 –min-alternate-fraction 0.2 –no-partial-observations`. The samples were compared against the gnomAD 2.1 database for detecting potential novel variants. We identified extremely rare (minor allele frequency [MAF] < 0.0001) and novel variants present in a minimum of three probands in known CHD-associated genes and genes known to be associated with cardiac development.<sup>35</sup>

### Human induced pluripotent stem cell lines

Four human induced pluripotent stem cell lines (hiPSCs) (HEL47.2, HEL24.3, HEL46.11, and HEL149.2) were obtained from the Biomedicum Stem Cell Center Core Facility. The cell lines were created by using retroviral/Sendai virus transduction of Oct3/4, Sox2, Klf4, and c-Myc, as described previously.<sup>36,37</sup> hiPSC line K1 was a kind gift from Anu Suomalainen-Wartiavaara. hiPSCs were maintained in Essential 8 media (A1517001, Thermo Fisher Scientific) on thin-coated Matrigel (354277, dilution 1:200; Corning). The cells were passaged using EDTA. The cells were routinely tested for mycoplasma with MycoAlert Mycoplasma Detection Kit (Lonza, LT07-218).

### scRNA-seq bioinformatics

Analysis was performed in R-studio using Seurat version 4.3.0. Cells with a minimum of 200 features, maximum of 8,000 features and <30% mitochondrial content were included. Normalization was carried out using “NormalizeData” and “ScaleData” and “FindVariableFeatures.” To integrate the data we used

“SelectIntegrationFeatures,” “FindIntegrationAnchors,” and “IntegrateData” functions. Principal-component analysis (PCA) was carried out on highly variable genes (dims = 1:30, Resolution = 0.2), these were used for uniform manifold approximation (UMAP). FindAllMarkers function was used to find differentially expressed genes. Established markers on The Human Protein Atlas and published literature were used to annotate cell types.

### RNA-seq bioinformatics

The data were analyzed using Chipster software.<sup>38</sup> Differential expression was calculated using DEseq2. Genes with adjusted *p* values of <0.05 for the log2fold-change were considered significant. Only genes with log2Fold-change on >0.25 were included. DAVID Bioinformatics Resources 6.8 was used for gene ontology (GO) analysis.<sup>39,40</sup>

### Zebrafish (*Danio rerio*) transgenesis and videomicroscopy

Vectors containing *ERBB2* WT and *ERBB2* c.1795C>T, as well as empty vectors with mCherry-CAAX (Figure S1) under myocardium-specific cmlc2-promoter were injected into 1–4 cell stage zebrafish embryos (casper or kdrl:EGFP line) using Nanoject II microinjector (Drummond Scientific). One day after injection, the dead and malformed embryos were removed, and embryos were cultured in E3-medium supplemented with 0.2mM 1-phenyl 2-thiourea (PTU) until analyzed. Injected embryos displaying mCherry-CAAX fluorescence were selected for phenotypic analyses (median percentage of cardiomyocytes expressing mCherry-CAAX was 24% [interquartile range 13%–36%, *n* = 52 embryos]). Embryos were anesthetized with MS-222 (200 mg/L) and allowed to acclimatize to room temperature for at least 30 min before videos were taken at four dpf using Zeiss AxioZoom stereomicroscope and imaging at 30 fps frame rate. Five- to 10-s movies were recorded from each embryo. After imaging, the zebrafish embryos of 4 dpf were euthanized under terminal tricaine (Ethyl 3-aminobenzoate methanesulfonate, 200 mg/L) anesthesia by fixation in 4% formaldehyde. Videos were analyzed with FIJI software.<sup>41</sup> Statistical analyses were done with GraphPad Prism 8 software.

## Results

A missense single-nucleotide variant (SNV) in *ERBB2* (chr17:39717377 C>T, NM\_004448.4:c.1795C>T, p.Arg599Cys (GRCh38), rs369903296) was identified in three unrelated probands with LVOTO defects (Figures 1A and 1B). All three of these probands were familial cases with multiple affected members. All three probands had severe phenotypes, and they were diagnosed either prenatally or during the first days of life (Proband of family 1: HLHS [including BAV, hypoplastic aortic arch, coarctation of the aorta, atrial septal defect, left superior vena cava]; Proband of family 2: Shone’s complex and ventricular septal defect [VSD] [including aortic valve stenosis, mitral stenosis (parachute valve), coarctation of the aorta]; Proband of family 3: HLHS [including mitral stenosis, BAV, aortic valve stenosis, and muscular ventricular septal defect]). We then identified the pres-

ence of the variant in the exome data of the family members of two probands where familial exomes were available (family 1 and family 2) and did targeted Sanger sequencing of the family members of the third proband (family 3) who was initially recruited as a singleton. In addition to the probands, the variant was found in all other affected family members in all families. The variant was also found in two unaffected family members in family 2, suggesting reduced penetrance (Figure 1A). The affected individuals did not have shared variants in known CHD genes or have any other identifiable genetic cause for their heart defects. The affected family members had less severe phenotypes than the probands, In family 1, the paternal grandfather; in family 2, the mother; and in family 3, the mother were all operated for coarctation of the aorta in childhood or early adulthood. In family 1, the father and in family 2, the maternal grandfather have not needed an operation. One asymptomatic variant carrier in family 3 has not been studied by echocardiogram. The penetrance of the variant was 72% (8 of 11) when the individual not studied by echocardiogram was presumed unaffected.

The chr17: 39717377 C>T (c.1795C>T) variant is present in heterozygotic form in seven subjects in GnomAD (v4.1.0, six Finnish Europeans and one non-Finnish European), with a total allele frequency of 0.00009372 in Finnish Europeans and 0.000004340 across all populations. The variant is not reported in Clinvar. It is predicted to be possibly damaging in PolyPhen and deleterious in SIFT, and it has a CADD score of 29.9 (GRCh37 v1.6). Multiple sequence alignment shows high conservation of the variant locus in *ERBB2* in multiple species (Figure 1C). In addition, the cysteine residue locations of the variant region are conserved in the four EGFR family members (Figure 1D).

### Other genetic findings in the study cohort

Three other individuals in the study cohort had pathogenic or likely pathogenic putative loss of function variants in *NOTCH1* (Table S1) and these results have been presented in a previous publication.<sup>24</sup> None of the other study individuals had pathogenic or likely pathogenic variants in other genes associated with CHD.

### The *ERBB2* p.Arg599Cys does not affect receptor tyrosine phosphorylation

As the variant results in an extra cysteine residue in the extracellular part of the *ERBB2* receptor close to the transmembrane region, we hypothesized that this could induce changes in the receptor function. We first investigated the functionality of the mutant *ERBB2* receptor by transfecting Cos7 cells with plasmid containing either wild-type (WT) *ERBB2* vector or *ERBB2* c.1795C>T vector. Western blot results show that *ERBB2* p.Arg599Cys can be phosphorylated at Tyr1284 at the same level, or even more, as the *ERBB2* WT (Figures S2A and S2B).

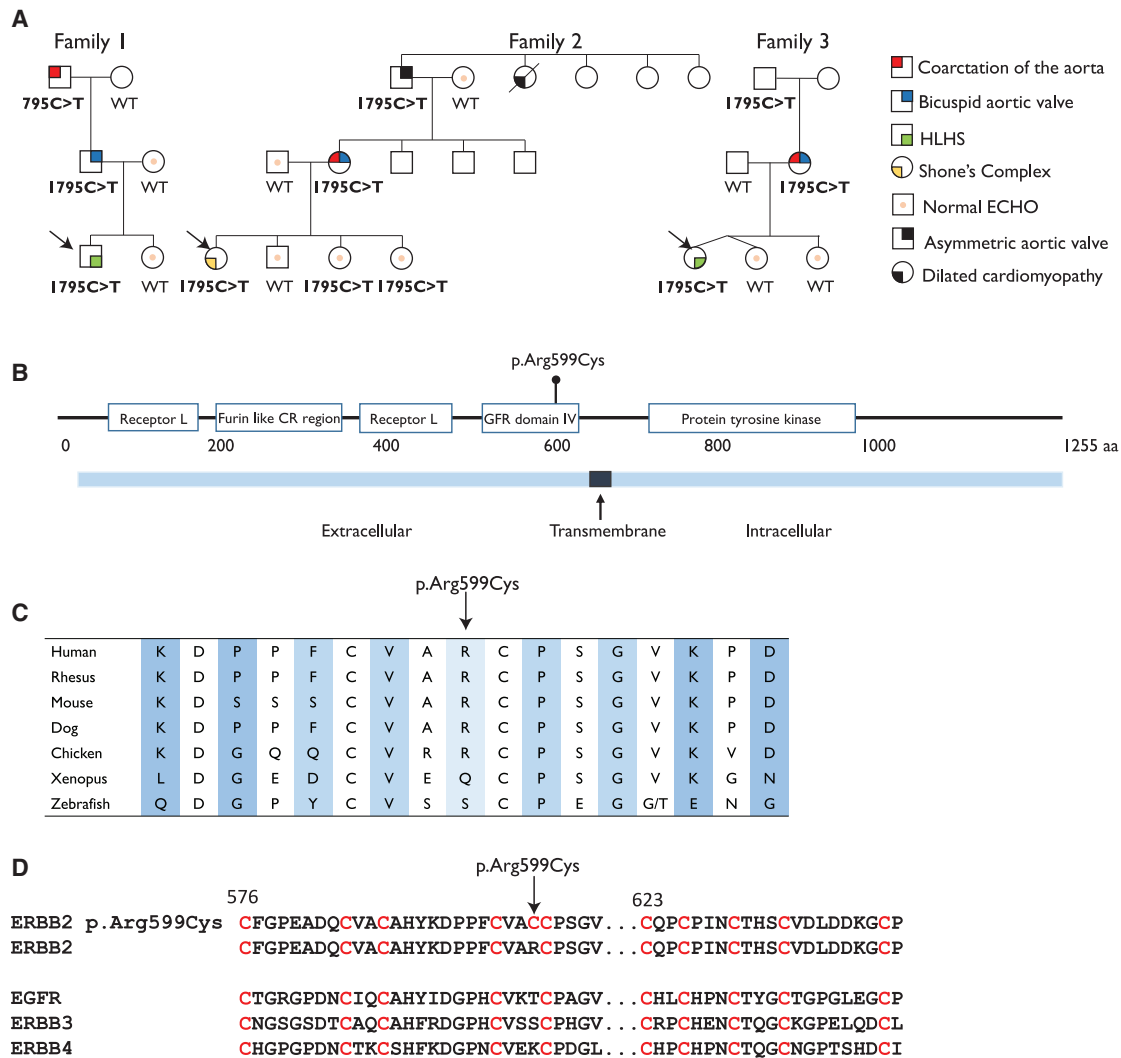


**Figure 1. ERBB2 c.1795C>T variant and pedigrees of the affected families**

(A) Pedigrees of the three affected families. Arrows indicate the probands in each family.

(B) The p.Arg599Cys variant is located in the extracellular GFR domain IV of ERBB2.

(C) ERBB2 protein sequence conservation around the variant site.

(D) Protein sequence alignment of the four members of the EGFR family and the ERBB2 p.Arg599Cys mutant showing conservation of the cysteine sites in the four WT receptors, and addition of an extra cysteine in the ERBB2 p.Arg599Cys mutant.

To confirm these findings in the cells of an individual with HLHS, we examined the phosphorylation of ERBB2 in hiPS-CMs from a person with the p.Arg599Cys variant and from healthy control hiPS-CMs. We acquired peripheral blood mononuclear cells from the proband of the family 1, created hiPSCs and differentiated them into cardiomyocytes (hereafter referred to as proband-hiPS-CMs). First, we ascertained that the variant allele is expressed in the proband-hiPS-CMs. Digital PCR results showed that in both hiPSCs and hiPSC-CMs the variant allele accounted for approximately 50% of the ERBB2 expression (Figure 2A). We then stimulated the cells with Neuregulin 1 and performed Simple Western with the Jess Automated Western Blot System. The results show similar relative phosphorylation in the proband-hiPS-CMs compared with the control hiPS-CMs (Figure 2B).

### The ERBB2 p.Arg599Cys receptor has different interaction partners compared with ERBB2 WT

We next hypothesized that the change from arginine to cysteine, which introduces a free cysteine in the transmembrane domain of the receptor, may affect dimerization, binding, and/or localization of the receptor.

We first tested this by gel electrophoresis and western blotting. Cos7 cells were transfected with ERBB2 WT or ERBB2 c.1795C>T plasmids and the cell lysates were run in gel electrophoresis with and without reducing agent DTT. Protein samples without DTT retain their disulfide bonds. The results show that there are significantly more ERBB2 disulfide bonds in the ERBB2 c.1795C>T transfected cells compared with the ERBB2 WT cells (Figures 2C and 2D).

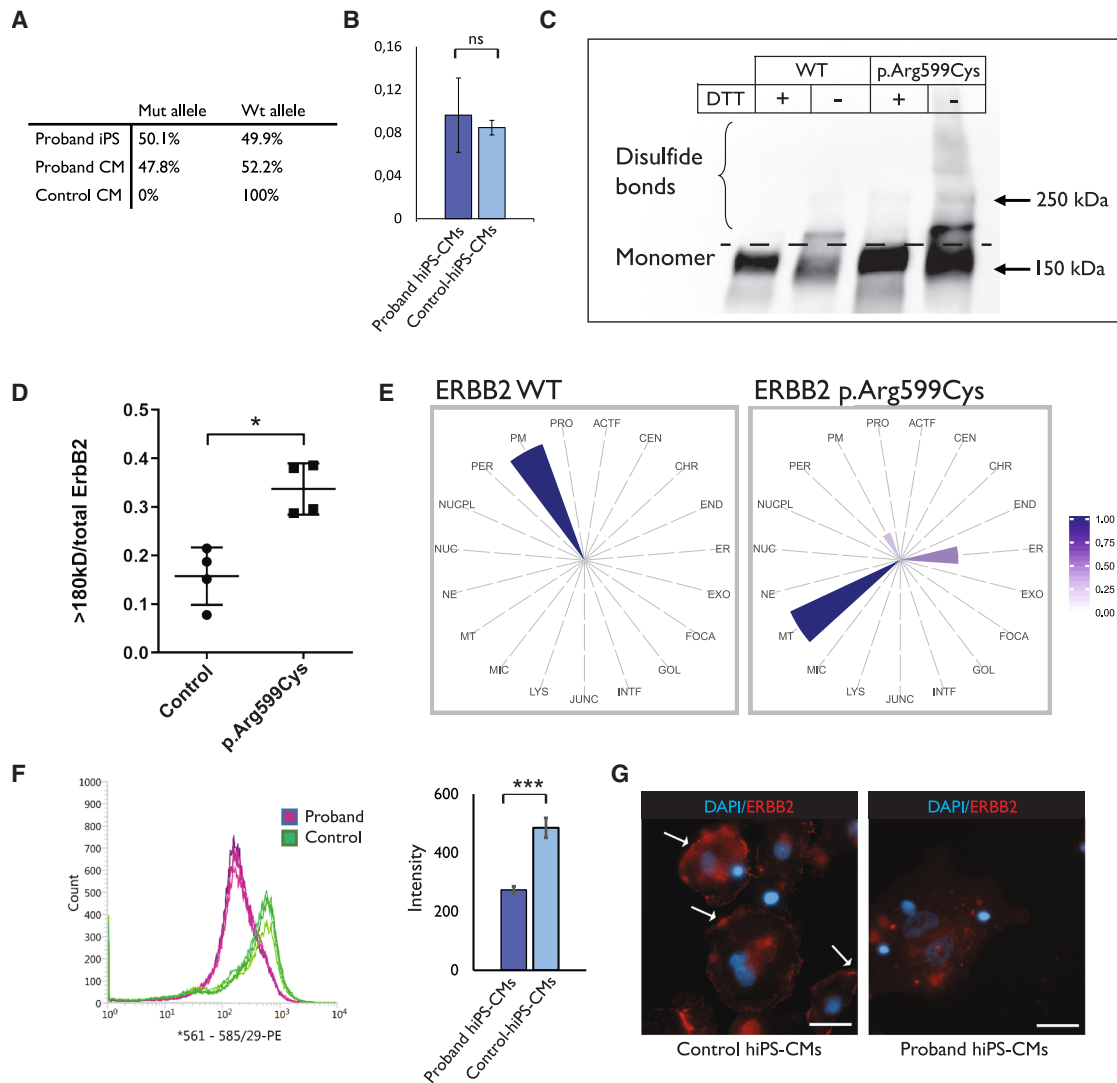


## Figure 2. ERBB2 p.Arg599Cys variant results in protein mislocalization

(A) Digital PCR confirms that the variant allele accounts for half of the ERBB2 expression levels in proband-hiPSCs (three technical replicates from one sample) and hiPS-CMs (three technical replicates from a representative sample of three different CM differentiations), whereas the hiPS-CMs from a control subject (HEL47.2) have 100% expression of the WT allele (three technical replicates from one sample).

(B) Simple western shows that there is no difference in the ERBB2 phosphorylation levels between proband hiPS-CMs and hiPS-CMs from a control subject (HEL47.2) (three replicates from one proband and one healthy hiPS-CM differentiation). Results are presented as mean with standard deviation.

(C) Cos-7 cells were transfected with either *ERBB2* WT or *ERBB2* c.1795C>T plasmid. Leaving out the reducing agent (DTT) from the western blot reveals the ERBB2-protein complexes that are larger due to intact disulfide bonds.

(D) Quantification of the disulfide bonds from the western blot shows higher amount of disulfide crosslinks in for the ERBB2 p.Arg599Cys receptor. Results are presented as mean with standard error of the mean (experiment was repeated four times with one replicate in each experiment).

(E) MS microscopy shows differences in the predicted cellular location for the ERBB2 WT and ERBB2 p.Arg599Cys receptor (results are from three replicates).

(F) Flow cytometry with a PE-conjugated antibody that recognizes the extracellular part of ERBB2, and quantification of the intensities in the proband hiPS-CMs and two control hiPS-CMs (experiment repeated three times) indicate reduced levels of ERBB2 in proband hiPS-CMs (\*\*\* $p < 0.005$ , Mann-Whitney statistical test). Results are presented as mean with standard deviation.

(G) Control hiPS-CMs have more ERBB2 staining in the plasma membrane compared with proband hiPS-CMs (representative images from two technical replicates from one staining). Arrows point to plasma membrane staining. Scale bar, 25  $\mu$ m.

To further understand the functional effect of the c.1795C>T variant we employed affinity purification combined with mass spectrometry (AP-MS) to examine and understand the stable interactions and proximity-depen-

dent biotin identification (BioID) to identify transient and close-range interactions. A comparative analysis of the high confidence interactors (HCIs) between the WT and p.Arg599Cys receptor revealed a significant difference

in the interacting partners (Table S2) and an enrichment of signaling pathways. Both loss of interacting partners (e.g., PLCG1, ELMO2), and novel interaction partners (e.g., PDIA4 and SSRP1) were observed in the p.Arg599Cys mutant. In addition, the p.Arg599Cys variant resulted in the reduction of interaction partners overall. Gene ontology (GO) analysis of the results indicated that the p.Arg599Cys mutant receptor had a reduction of interaction partners specifically in the ERBB2 and its downstream PI3K-Akt signaling pathway (e.g., ERBB4) (Figure S3).

### ERBB2 p.Arg599Cys receptor interacts with proteins in endoplasmic reticulum

To gain a deeper understanding of the potential compartment-specific localization of ERBB2, we utilized our recently developed MS microscopy system with the BioID data.<sup>42</sup> This system combines quantitative interactome profiling with microscopy techniques to accurately map the cellular distribution of ERBB2. The ERBB2 WT receptor was identified to be localized mainly at the plasma membrane, as expected. Interestingly, the ERBB2 p.Arg599Cys receptor was predicted to localize mostly to mitochondria and endoplasmic reticulum (ER) based on its interaction partners (Figure 2E).

To confirm these findings, proband hiPS-CMs and hiPS-CMs from two healthy individuals (HEL24.3, HEL47.2) were then stained with an ERBB2 antibody that binds to the extracellular part of the receptor and the cells were analyzed with flow cytometry. Indeed, the results were consistent with the MS microscopy findings showing that the proband hiPS-CMs had approximately half of the staining intensity of the control cells on the cell membrane, further supporting the hypothesis that the mutant protein localizes mostly intracellularly (Figure 2F).

In addition to flow cytometry, we also performed immunofluorescence staining of the proband hiPS-CMs and control hiPS-CMs. In the proband hiPS-CMs there was less plasma membrane staining of ERBB2 (Figure 2G). We also transduced ERBB2 knockout hiPS-endothelial cells (hiPS-ECs) with either ERBB2 WT lentivirus or ERBB2 c.1795C>T lentivirus. Immunofluorescence staining for ERBB2 and PDI after transduction showed prominent ER localization in mostly ERBB2 c.1795C>T transduced hiPS-ECs (Figure S4).

### Zebrafish embryos expressing the ERBB2 p.Arg599Cys have impaired cardiac contractility and increased cardiac wall thickness

Next, we examined the functional role of the ERBB2 p.Arg599Cys receptor during heart development. Zebrafish embryos were injected with a plasmid containing either ERBB2 WT or ERBB2 c.1795C>T together with membrane-localized mCherry-CAAX reporter to enable visualization of the cardiomyocytes with integrated transgene (Figure S1). Two control groups, one with an empty vector and one with non-injected embryos, were included. There was no difference in the fractional short-

ening between ERBB2 WT injected, vector injected, or non-injected hearts (Figure 3A), showing that the plasmid injection itself or human ERBB2 WT overexpression did not affect cardiac function. However, zebrafish embryos injected with the ERBB2 c.1795C>T plasmid demonstrated significantly lower fractional shortening compared with the ERBB2 WT injected embryos and the two control groups (Figure 3A), indicating compromised function of the heart caused by the p.Arg599Cys variant. In searching for underlying physical defects in the heart, we discovered that the cardiac wall was significantly thicker in the ERBB2 p.Arg599Cys embryos, measured from the brightfield movies (Figure 3B). By using whole-mount actin staining we could determine that specifically the myocardium was thicker in the ERBB2 p.Arg599Cys embryos compared with ERBB2 WT embryos (Figure 3C). To determine whether the thickening of the myocardium was a result from hyperplasia or hypertrophy of the cells, the number of myocardial nuclei were counted, and the area of the cells was determined from the mCherry-CAAX positive myocardial cells. The results showed no difference in the number of nuclei, indicating no hyperplasia (Figure 3D). mCherry-CAAX staining, in turn, revealed increased surface area of the mutant cells (Figures 3E and 3F), confirming that the thickening of the myocardium was due to the hypertrophy of the cardiomyocytes.

### ERBB2 p.Arg599Cys proband hiPSC-derived cardiomyocytes and endothelial cells have aberrant expression of genes related to cardiovascular system development

HiPS cells derived from the proband of family 1 with the ERBB2 c.1795C>T, p.Arg599Cys variant and from four healthy controls (HEL24.3, HEL47.2, HEL46.11, K1) were differentiated into cardiomyocytes and single-cell RNA sequencing (scRNA-seq) was performed when the cells were approximately 35 days old. Six clusters were identified in the UMAP (Figure 4A), with all clusters expressing cardiomyocyte-specific genes (Figure 4B), demonstrating efficient differentiation and selection. Pathway analysis revealed altered expression of genes related to heart development, muscle contraction, cardiac muscle hypertrophy, and stress responses in the proband hiPS-CMs (Figure 4C; Table S3). Compared with the healthy cells, the proband hiPS-CMs had significantly lower expression of cardiac genes such as MYH6, NPPA, and NPPB and higher expression of MYH7 (Figure 4D; Table S3). Finally, the proband hiPS-CMs had lower expression of many genes related to oxidative stress (Figure 4E; Table S3). In corroboration with the protein-protein interaction data, several genes associated with the PI3K/Akt pathway (such as ANKRD1 and NES) were downregulated in the proband hiPS-CMs compared with controls (Table S3).

As proper heart development involves intimate cross-talk between endothelial/endocardial cells and cardiomyocytes, we studied the effect of the ERBB2 c.1795C>T variant on endothelial cells. The proband-hiPSCs and cells

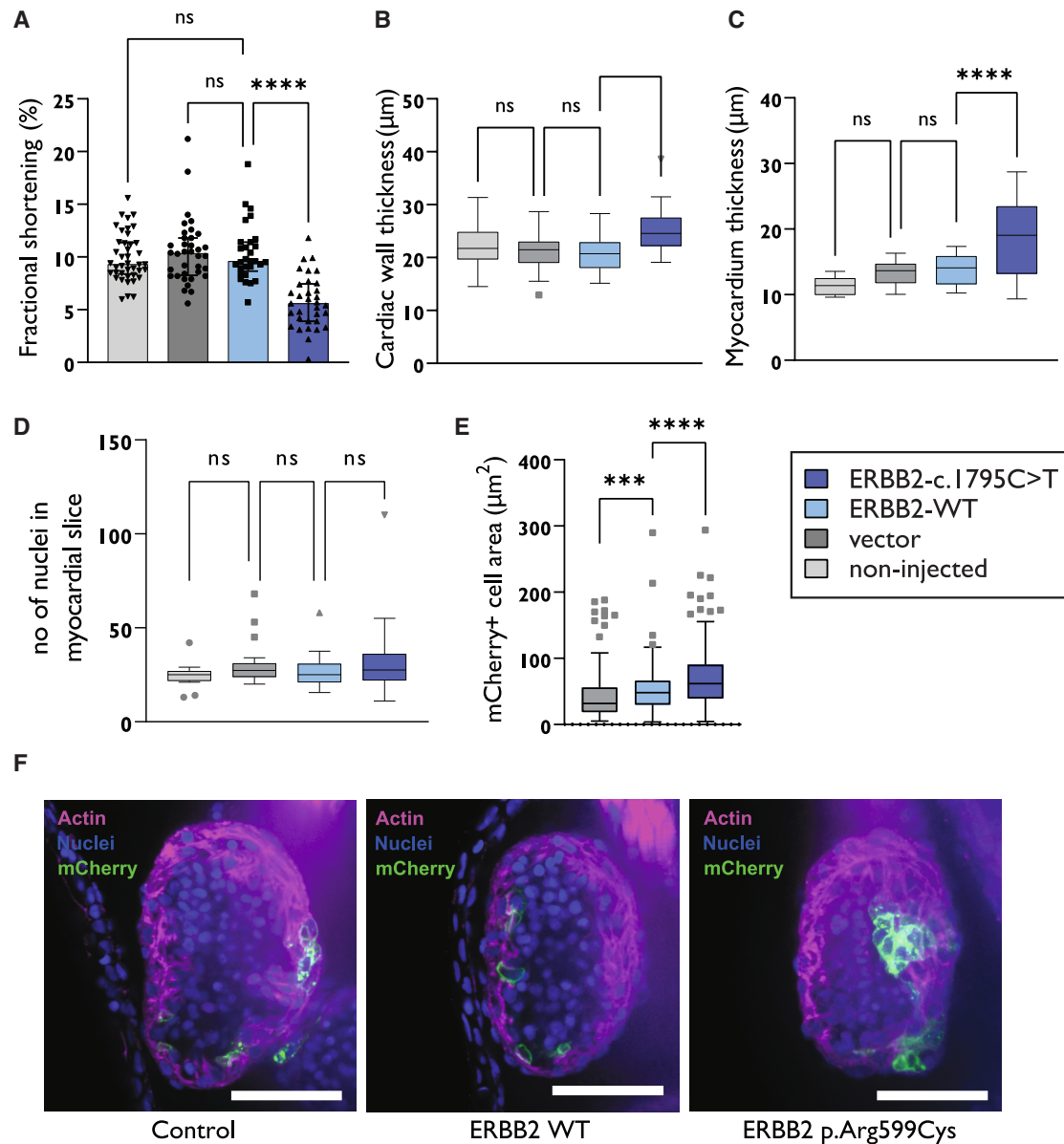


### Figure 3. ERBB2 variant results in compromised heart function in zebrafish

(A) Fractional shortening of the heart of the zebrafish embryos injected with the *ERBB2* c.1795C>T plasmid (33 embryos), *ERBB2* WT plasmid (29 embryos), empty vector (36 embryos), and no injection (41 embryos) indicate decreased pump function in the zebrafish embryos injected with the *ERBB2* c.1795C>T plasmid. Median with interquartile range is presented.

(B) Increased cardiac wall thickness as measured from brightfield videos (non-injected,  $n = 42$  embryos; vector,  $n = 39$  embryos; *ERBB2* WT,  $n = 30$  embryos; *ERBB2* c.1795C>T,  $n = 33$  embryos).

(C) Increased myocardium thickness measured by phalloidin staining was seen in the zebrafish embryos injected with the *ERBB2* c.1795C>T plasmid (uninjected,  $n = 18$  embryos; vector,  $n = 22$  embryos; *ERBB2* WT,  $n = 22$  embryos; *ERBB2* c.1795C>T,  $n = 22$  embryos).

(D) No differences in the number of myocardial nuclei within the four experimental groups was seen (14 uninjected embryos, 22 empty vector embryos, 20 WT *ERBB2* embryos, 19 c.1795C>T embryos). Myocardium was identified based on anatomical location and phalloidin staining.

(E) Myocardial cell area measured by membrane localized mCherry-CAAX staining in each group indicated slightly enlarged cells in the zebrafish embryo injected with the *ERBB2* WT (212 cardiomyocytes from 16 embryos), *ERBB2* c.1795C>T plasmid (262 cardiomyocytes from 20 embryos) or only empty vector injected embryos (151 cardiomyocytes from 19 embryos).

(F) Example images of phalloidin staining of the heart. The ventricle lumen is filled with red blood cells (zebrafish red blood cells are nucleated) and myocardium identified with phalloidin staining. Scale bar, 50 μm. Statistical tests have been done using the Kruskal-Wallis test, \*\*\*\* $p < 0.0001$ , \*\*\* $p < 0.001$ . (B)–(D) are presented as Tukey Box and Whiskers.

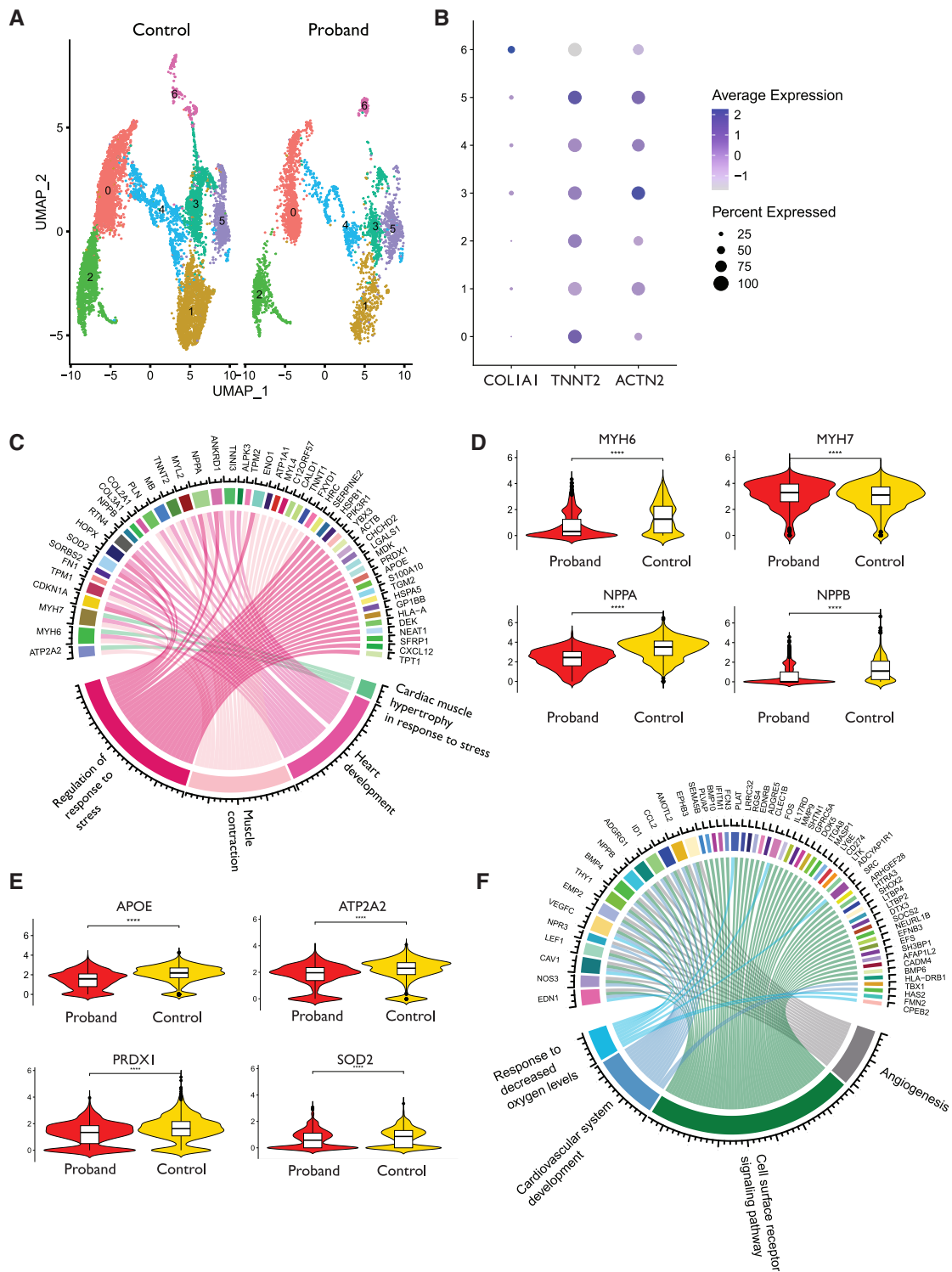


**Figure 4. Proband and control hiPS-CM and hiPS-EC transcriptomics**

(A) Uniform Manifold Approximation and Projection (UMAP) of proband hiPS-CMs and healthy control hiPS-CMs. The samples (one replicate each) consist of one proband hiPS-CM sample (from family 1 proband) and four control samples combined.

(B) Dot plot shows clusterwise expression of cardiomyocyte marker genes *TNNT2* and *ACTN2* and the fibroblast marker *COL1A1*.

(C) Circos plot of pathways that are differentially expressed in proband hiPS-CMs according to GO analysis.

(D and E) Violin plots presenting the expression levels of (D) heart development and (E) oxidative stress-related genes in proband-hiPS-CMs and control hiPS-CMs.

(F) Circos plot of pathways that are differentially expressed in proband-hiPS-ECs as compared with hiPS-ECs of healthy controls. Samples consist of two replicates from the proband hiPS-ECs and two replicates from three control hiPS-ECs. For statistical tests, false discovery rate has been applied.

from three healthy individuals (HEL47.2, HEL24.3, K1) were differentiated into ECs, and two independent differentiation batches were analyzed with whole-genome RNA sequencing. There were 198 repeatedly differentially expressed genes between the proband hiPS-ECs and control hiPS-ECs (Table S3). The proband hiPS-EC samples clustered together away from the control samples, demonstrating reproducibility between the two independent differentiations and differences in the transcriptome between the healthy and proband cells (Figure S5). Repressed expression in genes related to cardiovascular system development, response to decreased oxygen levels, programmed cell death, cell surface signaling pathway, and angiogenesis was observed, including genes such as *NPPB*, *NOS3*, *SRC*, and *BMP10* (Figure 4F; Table S3).

## Discussion

We have identified a rare *ERBB2* missense variant c.1795C>T, p.Arg599Cys in three unrelated Finnish families with LVOTO defects. The variant caused protein mislocalization, striking differences in binding partners, altered transcriptomics in proband-derived hiPS-cardiomyocytes and hiPS-endothelial cells, and resulted in developmental defects in zebrafish embryo hearts, providing functional evidence for the *ERBB2* variant to be associated with the phenotype.

*ERBB2* (Erb-B2 Receptor Tyrosine Kinase) encodes one of four members of the epidermal growth factor (EGF) receptor family of receptor tyrosine kinases. ErbB receptor dimerization by neuregulin leads to tyrosine kinase activation, which plays a vital role in embryogenesis.<sup>29,43</sup> *ERBB2* has not been previously associated with CHDs in humans even though its essential role in cardiac morphogenesis, especially in cardiac wall trabeculation, is well established in animal models.<sup>29,44–46</sup> In addition, the importance of *ERBB2* signaling in the adult heart has been demonstrated when trastuzumab, an *ERBB2* monoclonal antibody used in breast cancer therapy, was shown to associate with increased left ventricular dysfunction when used in combination with anthracyclines.<sup>47</sup>

Unlike other EGF receptors, *ERBB2* has no ligand binding domain of its own and therefore cannot bind growth factors. However, it does bind tightly to other ligand-binding EGF receptor family members to form heterodimers, enhancing kinase-mediated activation of downstream signaling pathways via receptor phosphorylation.<sup>48</sup> Our results show that the change of arginine to cysteine in the *ERBB2* p.Arg599Cys mutant does not affect the tyrosine phosphorylation of the receptor. As the phenotype could not be explained by defective phosphorylation, we explored the interactions of the *ERBB2* p.Arg599Cys mutant receptor with other proteins. The results revealed that the mutant receptor has overall fewer and different binding partners compared with the WT receptor. According to the MS microscopy, the *ERBB2* p.Arg599Cys mutant

receptors binding partners localize to the mitochondria and endoplasmic reticulum (ER), and in line with this result, the proband-hiPS-CMs had roughly 50% reduced expression of *ERBB2* on the plasma membrane compared with healthy cells. Immunofluorescence staining of hiPS-ECs transduced with *ERBB2* WT or *ERBB2* c.1795C>T show that *ERBB2* p.Arg599Cys co-localizes with ER-marker PDI. As no specific co-localization with mitochondrial marker TOMM20 was found for the mutant receptor (data not shown), we speculate that since the MS microscopy interactions are based on transient interactions, the *ERBB2* p.Arg599Cys localization in ER positions it in close contact with mitochondria as well. Quantification of immunofluorescence images show results consistent with changes in localization, although quantification is hindered by variable intensity of transduced *ERBB2* and quantification from 2D image disallowing complete separation of plasma membrane staining from intracellular staining (resulting in some plasma membrane staining being accounted into ER staining), possibly explaining the smaller difference in localization observed in staining compared with flow cytometry. Altogether, these results indicate that the p.Arg599Cys variant leads to mislocalization of the protein intracellularly. The change in binding partners may be due to the free cysteine allowing the formation of an extra cysteine bond, or due to changes in the folding of the protein. The extra cysteine may also contribute to changes in protein-protein interaction via non-covalent interactions involving the sulfur atoms of the cysteine residue.<sup>49</sup> Although the cytosol as a reducing environment is not conducive to formation of disulfide bonds,<sup>50,51</sup> disulfide bonds can be formed in the ER and mitochondria.<sup>52</sup> It has been reported that *ERBB2* also localizes within the mitochondria of both cancer cells and other diseases.<sup>53</sup>

GO results from the protein-protein interaction assay indicate overall reduction of *ERBB2* and receptor tyrosine kinase signaling in cells with the *ERBB2* p.Arg599Cys receptor. The GO results and transcriptomics data also indicate reduced interaction with the PI3K-PKB/Akt pathway, which is one of the downstream signaling pathways of the *ERBB2* receptor.<sup>54–56</sup> Thus, as the mutant receptor phosphorylation was not deficient, it is likely that protein mislocalization and/or altered binding partners cause the impaired *ERBB2* signaling. Defective *ERBB2* signaling may lead to e.g., reduced proliferation of cells, as proliferation-related GO terms are only found in the WT *ERBB2* interactions.

Many of the PI3K-PKB/Akt pathway proteins with reduced interaction with the *ERBB2* p.Arg599Cys receptor have important roles in heart development or function. *PRKCI* is required for heart trabeculation in mice,<sup>57</sup> *PIK3R2* regulates heart size and hypertrophy in mice,<sup>58</sup> *PIK3CB* promotes CM proliferation and survival in neonatal rat CMs<sup>59</sup> and *PRKCA* regulates heart contractility in mice.<sup>60</sup> In addition, the *ERBB2* p.Arg599Cys receptor had reduced interaction with proteins such as *SOS1*, *PTPN11*, and *CBL*, which have been associated

with syndromic CHDs<sup>61–63</sup> and MICOS13, DTNA, and EMC1 which have been associated with non-syndromic CHDs.<sup>64–66</sup> In addition, the mutant receptor has lost interaction with FRS2, which is required for outflow tract morphogenesis.<sup>67</sup> Loss of interaction with these proteins that are implicated to be important for heart development may contribute to observed heart defects in the individuals with the mutant receptor.

To study the functional effect of the ERBB2 p.Arg599Cys mutant receptor *in vivo*, we used zebrafish, as they are a commonly used model for heart development and regeneration.<sup>68,69</sup> Interestingly, expression of the mutant ERBB2 in zebrafish embryo hearts led to cardiomyocyte hypertrophy, increased cardiac wall thickness, and impaired fractional shortening demonstrating that the presence of the mutant receptor induces functional defects during heart development. Although we did not observe significant changes in the number of transgenic cardiomyocytes in the zebrafish model, the existence of mild hyperplasia cannot be completely ruled out. Animal models of HLHS have shown that intrinsic myocardial defects are associated with HLHS,<sup>70,71</sup> and a recent study in zebrafish demonstrated that *rbfox* mediated reduction in pump function led to compromised development of the valves and aorta.<sup>71</sup> Thus, our findings in the zebrafish recapitulate this predisposition for outflow tract obstruction development.

When modeling HLHS at the cellular level, transcriptomic and functional studies on hiPS-CMs derived from individuals with HLHS have shown impaired differentiation,<sup>72,73</sup> less organized sarcomere structure,<sup>72–74</sup> and reduced contractility<sup>75</sup> that likely are associated with the compromised pump function seen in animal models of HLHS. Our results were in line with these studies. The transcriptomic analyses of proband hiPSC-CMs provide evidence that several genes and pathways related to heart and cardiovascular system development were affected in proband hiPS-CMs. Among the downregulated genes were two important sarcomere proteins, MYH6, which has been associated with HLHS,<sup>74</sup> and TNNI3, which has been associated with dilated, hypertrophic, and familial restrictive cardiomyopathy.<sup>76–78</sup> Reduced expression of *TNNI3* in HLHS hiPS-CMs has also been demonstrated in a previous study.<sup>72</sup> In contrast, gene expression of the sarcomere protein *MYH7* was increased in the proband hiPS-CMs, and interestingly, increased *MYH7* expression has been shown in atrial and ventricular tissues of HLHS subjects, and in hiPS-CMs derived from individuals with HLHS.<sup>74</sup> Moreover, similar increases of *TNNT2* and *MYL2* expression in HLHS-hiPS-CMs observed in our study have been documented previously.<sup>74</sup>

Intrinsic endocardial defects contributing to abnormal valve formation have been associated as a potential mechanism underlying HLHS,<sup>79</sup> and loss of *ErbB2* in mouse coronary endothelial cells during development has been associated with improper patterning of coronary vasculature,<sup>80</sup> demonstrating its important role in endothelial

cells in cardiac development. Intimate crosstalk between ECs and CMs is essential during cardiac development. Therefore, we also studied the proband hiPSC-ECs using RNA-seq in comparison with cells from healthy controls.

The transcriptomic analyses of proband-hiPS-ECs provide evidence that several genes and pathways related to heart and cardiovascular system development were affected in the proband-hiPS-ECs. Expression of *BMP10* was downregulated in proband-hiPS-ECs. Previous research has highlighted the significance of BMP10 in preserving the expression of genes crucial for cardiac development, including *NKX2.5*, which has been identified as being associated with HLHS.<sup>81,82</sup> Additionally, BMP10-null mice have been shown to have defects in cardiomyocyte proliferation and trabeculation.<sup>82</sup> These findings further support the theory that ECs have a role in the development of HLHS.

Abnormal response to oxidative stress is associated with CHDs.<sup>83–86</sup> A recent study showed reduced mitochondrial respiration and oxidative metabolism in HLHS hiPS-CMs compared with healthy controls potentially contributing to reduced contractility.<sup>75</sup> Several oxidative stress and metabolic genes were downregulated both in proband-hiPS-ECs and -CMs compared with healthy controls. The role of ERBB2 in endothelial ischemic conditions has been demonstrated in a mouse model, where ERBB2-signaling was shown to facilitate the recruitment of SRC. This recruitment subsequently activated NOS3 through NRG1, leading to enhanced myocardial perfusion by elevating nitric oxide production and promoting vasorelaxation.<sup>87</sup> Interestingly, decreased expression was observed for both *SRC* and *NOS3* in proband hiPS-ECs. NOS3-deficiency has demonstrated an association with a bicuspid aortic valve in mice. This connection possibly arises from the role of the valvular endothelium in fine tuning the developmental process through mechanisms like shear stress and other luminal events.<sup>88</sup> Moreover, reduced expression in metabolic genes including *ENO1*, *SOD2*, and *SOD3* was observed in the proband-hiPS-CMs. These genes have been shown to provide protection under hypoxic and oxidative stress.<sup>75,89,90</sup>

ERBB2 variants have not previously been associated with CHD in humans, but one study has reported copy number variants including an *ERBB2* duplication in an individual with total anomalous pulmonary venous return and in an individual with Tetralogy of Fallot.<sup>91</sup> However, no further experiments were performed to validate the findings or to further investigate the potential role of *ERBB2* in CHDs.

While most persons with the *ERBB2* c.1795C>T variant had CHD, there were two persons with this variant who had normal echocardiographic findings and one person without reported cardiac symptoms but in whom no echocardiographic data were available. This is not unexpected, as reduced penetrance has been associated with monogenic CHD in multiple studies. For example, *NOTCH1* haploinsufficiency is a well-known cause of

CHDs with a penetrance reported to be about 75%,<sup>22,24</sup> which is similar to our observation for *ERBB2*. In addition, our study clearly demonstrated the variable expressivity associated with CHDs,<sup>22,24</sup> as the cardiac abnormalities ranged from BAV and CoA to HLHS and Shone's complex. Of note, the phenotype severity seemed to worsen with consecutive generations. This could be due to accumulation of additional predisposing variants, or environmental triggers. However, this can also depend on selection of study subjects, as our study cohort comprised on average more severe pediatric individuals and thus led to ascertainment bias.

Previous research shows that total *Erb2* deletion in mice leads to lethal cardiac malformations early during development,<sup>29</sup> while mice with conditional knockout of *Erb2* in ventricular myocytes show normal cardiac morphogenesis at birth and survive to adulthood.<sup>92</sup> However, in adulthood these mice show features of dilated cardiomyopathy including biventricular enlargement, decreased cardiac wall thickness, and decreased fractional shortening.<sup>92</sup> Thus, it seems clear that the role of *ERBB2* signaling in the adult heart is different from its role during embryogenesis, and that during development, *ERBB2* signaling is essential in several different cell types. Nevertheless, the recent observation that reduced ventricular contractility led to compromised development of the valves and aorta in zebrafish<sup>71</sup> supports the hypothesis that intrinsic myocardial defects, possibly mediated by additional cell types such as endocardial or endothelial cells, are causal for the phenotype observed in our affected study subjects. Of note, the study subjects in this cohort did not have heart failure or reduced cardiac function beyond what is expected for the phenotype at the time of the assessment, so it can be speculated that one normally functioning allele of *ERBB2* is sufficient for cardiac function in the study individuals after birth.

Taken together, our results provide strong evidence for association of the *ERBB2* variant with LVOTO defects. The *ERBB2* c.1795C>T variant was present in all affected members of three unrelated families with CHDs in multiple generations. The variant is reported in gnomAD in heterozygous form in six Finnish individuals, and only one non-Finnish European, suggesting that the variant is a rare missense variant in the Finnish population. Functional analysis of the mutant receptor demonstrated dramatic changes in the binding partners and cellular localization of the receptor. Finally, expression of the mutant allele caused compromised heart function in the zebrafish embryos. Further analysis on the exact mechanisms of the mutant protein at the cellular level will provide more information on the pathogenic events leading to CHD during cardiac development.

## Data and code availability

- The RNA sequencing data underlying this article are available in GEO under accession numbers GEO: GSE247858 and GEO:

GSE194103. The mass spectrometry data are available at MassIVE with dataset ID MassIVE: MSV000093153 (<https://massive.ucsd.edu/ProteoSAFe/dataset.jsp?task=1bfd8a81ba14008af86bf3280f7506f>).

- The exome sequencing data are not shared publicly because they consist of individual genotypes for minors. Data are available from the Helsinki University Hospital's Institutional Data Access/Ethics Committee for researchers who meet the criteria for access to confidential data.

## Acknowledgments

This study has been funded by the Academy of Finland (297245, 331405), the Finnish Medical Foundation, Foundation for Pediatric Research (Helsinki, Finland), The Finnish Cultural Foundation (Helsinki, Finland), Finnish Foundation for Cardiovascular Research (Helsinki, Finland), Sigrid Juselius Foundation, University of Helsinki, Helsinki University Hospital, Orion Research Foundation, Päivikki and Sakari Sohlberg Foundation, and Aarne Koskelo Foundation. Exome sequencing and data analysis were provided by the University of Washington Center for Rare Disease Research (UW-CRDR) with support from NHGRI grants U01 HG011744, UM1 HG006493, and U24 HG011746. The content is solely the responsibility of the authors and does not necessarily represent the official views of the National Institutes of Health. We thank Ilse Paetau and Katja Salo for their help in laboratory experiments and administrative support. We thank Kari Alitalo, Tanja Laakkonen, and Seppo Kaijalainen for help with the *ERBB2* c.1795C>T plasmid. We thank Professor Anu Suomalainen-Wartiavaara, Professor Timo Otonkoski, and Docent Ras Trokovic for the iPSC cells. We thank Michael Jeltsch for providing VEGF for the experiments. We thank Zebrafish Core and Cell Imaging Core (both Turku Bioscience Center, University of Turku, and Åbo Akademi University, supported by Biocenter Finland) for instrumentation and services. scRNA-seq service was performed at FIMM Single-Cell Analytics unit, RNA-seq at Biomedicum Functional Genomics Unit and imaging at the Biomedicum Imaging Unit, all supported by HiLIFE and Biocenter Finland at the University of Helsinki. We acknowledge the HiLife Flow Cytometry Unit, University of Helsinki and Biomedicum Virus Core Unit (BVC), University of Helsinki.

## Author contributions

Conceptualization: E.H., R.K., M.A., and J.R.P.; data curation: A.R., M.B., M.A., I.P., S.E., I.C., J.X.C., and M.J.B.; formal analysis: S.E., M.B., A.R., I.P., M.A., and I.C.; funding acquisition: E.H., R.K., M.A., and M.J.B.; investigation: M.A., S.E., I.P., I.C., J.V., and D.B.; methodology: M.A., S.E., I.P., and D.B.; project administration: E.H. and R.K.; resources: E.H., R.K., I.P., M.V., J.X.C., and M.B.; software: S.E., I.C., M.B., and A.R.; supervision: E.H., R.K., I.P., and M.V.; visualization: M.A., S.E., I.P., J.V., and I.C.; writing – original draft: M.A., S.E., E.H., and R.K.; writing – review & editing: E.H., R.K., I.P., M.V., M.B., I.C., J.V., D.B., A.R., T.O., J.C., M.J.B., and J.R.P.

## Declaration of interests

The authors declare no competing interests.

## Supplemental information

Supplemental information can be found online at <https://doi.org/10.1016/j.xhgg.2025.100446>.

## Web resources

<http://www.omim.org/>

<https://massive.ucsd.edu/ProteoSAFe/dataset.jsp?task=1fbfd8a81ba14008af86bf3280f7506f>

Received: July 16, 2024

Accepted: April 30, 2025

## References

1. Kerstjens-Frederikse, W.S., Du Marchie Sarvaas, G.J., Ruiter, J. S., Van Den Akker, P.C., Temmerman, A.M., Van Melle, J.P., Hofstra, R.M.W., and Berger, R.M.F. (2011). Left ventricular outflow tract obstruction: should cardiac screening be offered to first-degree relatives? *Heart* 97, 1228–1232.
2. Oyen, N., Boyd, H.A., Carstensen, L., Sondergaard, L., Wohlfahrt, J., and Melbye, M. (2022). Risk of Congenital Heart Defects in Offspring of Affected Mothers and Fathers. *Circ. Genom. Precis. Med.* 15, e003533.
3. Foffa, I., Ait Ali, L., Panesi, P., Mariani, M., Festa, P., Botto, N., Vecoli, C., and Andreassi, M.G. (2013). Sequencing of NOTCH1, GATA5, TGFBR1 and TGFBR2 genes in familial cases of bicuspid aortic valve. *BMC Med. Genet.* 14, 44.
4. Gifford, C.A., Ranade, S.S., Samarakoon, R., Salunga, H.T., de Soysa, T.Y., Huang, Y., Zhou, P., Elfenbein, A., Wyman, S.K., Bui, Y.K., et al. (2019). Oligogenic inheritance of a human heart disease involving a genetic modifier. *Science* 364, 865–870.
5. Schulkey, C.E., Regmi, S.D., Magnan, R.A., Danzo, M.T., Luther, H., Hutchinson, A.K., Panzer, A.A., Grady, M.M., Wilson, D.B., and Jay, P.Y. (2015). The maternal-age-associated risk of congenital heart disease is modifiable. *Nature* 520, 230–233.
6. Basu, M., Zhu, J.Y., LaHaye, S., Majumdar, U., Jiao, K., Han, Z., and Garg, V. (2017). Epigenetic mechanisms underlying maternal diabetes-associated risk of congenital heart disease. *JCI Insight* 2, e95085.
7. Chapman, G., Moreau, J.L.M., I, P.E., Szot, J.O., Iyer, K.R., Shi, H., Yam, M.X., O'Reilly, V.C., Enriquez, A., Greasby, J.A., et al. (2020). Functional genomics and gene-environment interaction highlight the complexity of congenital heart disease caused by Notch pathway variants. *Hum. Mol. Genet.* 29, 566–579.
8. Helle, E., and Priest, J.R. (2020). Maternal Obesity and Diabetes Mellitus as Risk Factors for Congenital Heart Disease in the Offspring. *J. Am. Heart Assoc.* 9, e011541.
9. Agopian, A.J., Goldmuntz, E., Hakonarson, H., Sewda, A., Taylor, D., Mitchell, L.E.; and Pediatric Cardiac Genomics Consortium (2017). Genome-Wide Association Studies and Meta-Analyses for Congenital Heart Defects. *Circ. Cardiovasc. Genet.* 10, e001449.
10. Bjornsson, T., Thorolfsson, R.B., Sveinbjornsson, G., Sulem, P., Norddahl, G.L., Helgadóttir, A., Gretarsdóttir, S., Magnúsdóttir, A., Danielsen, R., Sigurdsson, E.L., et al. (2018). A rare missense mutation in MYH6 associates with non-syndromic coarctation of the aorta. *Eur. Heart J.* 39, 3243–3249.
11. Cordell, H.J., Bentham, J., Topf, A., Zelenika, D., Heath, S., Mamasoula, C., Cosgrove, C., Blue, G., Granados-Riveron, J., Setchfield, K., et al. (2013). Genome-wide association study of multiple congenital heart disease phenotypes identifies a susceptibility locus for atrial septal defect at chromosome 4p16. *Nat. Genet.* 45, 822–824.
12. Lahm, H., Jia, M., Dressen, M., Wirth, F., Puluca, N., Gilsbach, R., Keavney, B.D., Cleuziou, J., Beck, N., Bondareva, O., et al. (2021). Congenital heart disease risk loci identified by genome-wide association study in European patients. *J. Clin. Investig.* 131, e141837.
13. Ye, Z., Wang, L., Yang, T., Chen, L., Wang, T., Chen, L., Zhao, L., Zhang, S., Zheng, Z., Luo, L., and Qin, J. (2019). Maternal Viral Infection and Risk of Fetal Congenital Heart Diseases: A Meta-Analysis of Observational Studies. *J. Am. Heart Assoc.* 8, e011264.
14. Jenkins, K.J., Correa, A., Feinstein, J.A., Botto, L., Britt, A.E., Daniels, S.R., Elixson, M., Warnes, C.A., Webb, C.L.; and American Heart Association Council on Cardiovascular Disease in the Young (2007). Noninherited risk factors and congenital cardiovascular defects: current knowledge: a scientific statement from the American Heart Association Council on Cardiovascular Disease in the Young: endorsed by the American Academy of Pediatrics. *Circulation* 115, 2995–3014.
15. Fisher, S.C., Van Zutphen, A.R., Werler, M.M., Lin, A.E., Romitti, P.A., Druschel, C.M., Browne, M.L.; and National Birth Defects Prevention Study (2017). Maternal Antihypertensive Medication Use and Congenital Heart Defects: Updated Results From the National Birth Defects Prevention Study. *Hypertension* 69, 798–805.
16. Helle, E.I.T., Biegley, P., Knowles, J.W., Leader, J.B., Pendergrass, S., Yang, W., Reaven, G.R., Shaw, G.M., Ritchie, M., and Priest, J.R. (2018). First Trimester Plasma Glucose Values in Women without Diabetes are Associated with Risk for Congenital Heart Disease in Offspring. *J. Pediatr.* 195, 275–278.
17. Persson, M., Razaz, N., Edstedt Bonamy, A.K., Villamor, E., and Cnattingius, S. (2019). Maternal Overweight and Obesity and Risk of Congenital Heart Defects. *J. Am. Coll. Cardiol.* 73, 44–53.
18. Ramakrishnan, A., Lee, L.J., Mitchell, L.E., and Agopian, A.J. (2015). Maternal Hypertension During Pregnancy and the Risk of Congenital Heart Defects in Offspring: A Systematic Review and Meta-analysis. *Pediatr. Cardiol.* 36, 1442–1451.
19. Oyen, N., Poulsen, G., Boyd, H.A., Wohlfahrt, J., Jensen, P.K., and Melbye, M. (2009). Recurrence of congenital heart defects in families. *Circulation* 120, 295–301.
20. Oyen, N., Poulsen, G., Wohlfahrt, J., Boyd, H.A., Jensen, P.K. A., and Melbye, M. (2010). Recurrence of discordant congenital heart defects in families. *Circ. Cardiovasc. Genet.* 3, 122–128.
21. Huntington, K., Hunter, A.G., and Chan, K.L. (1997). A prospective study to assess the frequency of familial clustering of congenital bicuspid aortic valve. *J. Am. Coll. Cardiol.* 30, 1809–1812.
22. Kerstjens-Frederikse, W.S., van de Laar, I.M.B.H., Vos, Y.J., Verhagen, J.M.A., Berger, R.M.F., Lichtenbelt, K.D., Klein Wassink-Ruiter, J.S., van der Zwaag, P.A., du Marchie Sarvaas, G.J., Bergman, K.A., et al. (2016). Cardiovascular

- malformations caused by NOTCH1 mutations do not keep left: data on 428 probands with left-sided CHD and their families. *Genet. Med.* *18*, 914–923.
23. Giusti, B., Sticchi, E., De Carlo, R., Magi, A., Nistri, S., and Pepe, G. (2017). Genetic Bases of Bicuspid Aortic Valve: The Contribution of Traditional and High-Throughput Sequencing Approaches on Research and Diagnosis. *Front. Physiol.* *8*, 612.
  24. Helle, E., Córdova-Palomera, A., Ojala, T., Saha, P., Potiny, P., Gustafsson, S., Ingelsson, E., Bamshad, M., Nickerson, D., Chong, J.X., et al. (2019). Loss of function, missense, and intronic variants in NOTCH1 confer different risks for left ventricular outflow tract obstructive heart defects in two European cohorts. *Genet. Epidemiol.* *43*, 215–226.
  25. Ison, H.E., Griffin, E.L., Parrott, A., Shikany, A.R., Meyers, L., Thomas, M.J., Syverson, E., Demo, E.M., Fitzgerald, K.K., Fitzgerald-Butt, S., et al. (2022). Genetic counseling for congenital heart disease - Practice resource of the National Society of Genetic Counselors. *J. Genet. Counsel.* *31*, 9–33.
  26. Wilde, A.A.M., Semsarian, C., Márquez, M., Sepehri Shamloo, A., Ackerman, M.J., Ashley, E.A., Back Sternick, E., Barajas-Martinez, H., Behr, E.R., Bezzina, C.R., et al. (2022). Expert Consensus Statement on the state of genetic testing for cardiac diseases. *Europace* *24*, 1307–1367.
  27. Kaariainen, H., Muilu, J., Perola, M., and Kristiansson, K. (2017). Genetics in an isolated population like Finland: a different basis for genomic medicine? *J. Commun. Genet.* *8*, 319–326.
  28. Hautala, J., Gissler, M., Ritvanen, A., Tekay, A., Pitkänen-Argillander, O., Stefanovic, V., Sarkola, T., Helle, E., Pihkala, J., Pätilä, T., et al. (2019). The implementation of a nationwide anomaly screening programme improves prenatal detection of major cardiac defects: an 11-year national population-based cohort study. *BJOG* *126*, 864–873.
  29. Lee, K.F., Simon, H., Chen, H., Bates, B., Hung, M.C., and Hauser, C. (1995). Requirement for neuregulin receptor erbB2 in neural and cardiac development. *Nature* *378*, 394–398.
  30. Negro, A., Brar, B.K., and Lee, K.F. (2004). Essential roles of Her2/erbB2 in cardiac development and function. *Recent Prog. Horm. Res.* *59*, 1–12.
  31. D'Uva, G., Aharonov, A., Lauriola, M., Kain, D., Yahalom-Ronen, Y., Carvalho, S., Weisinger, K., Bassat, E., Rajchman, D., Yifa, O., et al. (2015). ERBB2 triggers mammalian heart regeneration by promoting cardiomyocyte dedifferentiation and proliferation. *Nat. Cell Biol.* *17*, 627–638.
  32. Honkoop, H., de Bakker, D.E., Aharonov, A., Kruse, F., Shakked, A., Nguyen, P.D., de Heus, C., Garric, L., Muraro, M.J., Shoffner, A., et al. (2019). Single-cell analysis uncovers that metabolic reprogramming by ErbB2 signaling is essential for cardiomyocyte proliferation in the regenerating heart. *Elife* *8*, e50163.
  33. Liu, J., Bressan, M., Hassel, D., Huisken, J., Staudt, D., Kikuchi, K., Poss, K.D., Mikawa, T., and Stainier, D.Y.R. (2010). A dual role for ErbB2 signaling in cardiac trabeculation. *Development* *137*, 3867–3875.
  34. Richter, F., Morton, S.U., Qi, H., Kitaygorodsky, A., Wang, J., Homsy, J., DePalma, S., Patel, N., Gelb, B.D., Seidman, J.G., et al. (2020). Whole Genome De Novo Variant Identification with FreeBayes and Neural Network Approaches. Preprint at bioRxiv. <https://doi.org/10.1101/2020.03.24.994160>.
  35. Yang, A., Alankarage, D., Cuny, H., Ip, E.K.K., Almog, M., Lu, J., Das, D., Enriquez, A., Szot, J.O., Humphreys, D.T., et al. (2022). CHDgene: A Curated Database for Congenital Heart Disease Genes. *Circ. Genom. Precis. Med.* *15*, e003539.
  36. Trokovic, R., Weltner, J., and Otonkoski, T. (2015). Generation of iPSC line HEL24.3 from human neonatal foreskin fibroblasts. *Stem Cell Res.* *15*, 266–268.
  37. Trokovic, R., Weltner, J., and Otonkoski, T. (2015). Generation of iPSC line HEL47.2 from healthy human adult fibroblasts. *Stem Cell Res.* *15*, 263–265.
  38. Kallio, M.A., Tuimala, J.T., Hupponen, T., Klemelä, P., Gentile, M., Scheinin, I., Koski, M., Käki, J., and Korpelainen, E.I. (2011). Chipster: user-friendly analysis software for microarray and other high-throughput data. *BMC Genom.* *12*, 507.
  39. Huang, D.W., Sherman, B.T., and Lempicki, R.A. (2009). Systematic and integrative analysis of large gene lists using DAVID bioinformatics resources. *Nat. Protoc.* *4*, 44–57.
  40. Sherman, B.T., Hao, M., Qiu, J., Jiao, X., Baseler, M.W., Lane, H.C., Imamichi, T., and Chang, W. (2022). DAVID: a web server for functional enrichment analysis and functional annotation of gene lists (2021 update). *Nucleic Acids Res.* *50*, W216–W221.
  41. Schindelin, J., Arganda-Carreras, I., Frise, E., Kaynig, V., Longair, M., Pietzsch, T., Preibisch, S., Rueden, C., Saalfeld, S., Schmid, B., et al. (2012). Fiji: an open-source platform for biological-image analysis. *Nat. Methods* *9*, 676–682.
  42. Liu, X., Salokas, K., Weldatsadik, R.G., Gawrylski, L., and Varjosalo, M. (2020). Combined proximity labeling and affinity purification-mass spectrometry workflow for mapping and visualizing protein interaction networks. *Nat. Protoc.* *15*, 3182–3211.
  43. Meyer, D., and Birchmeier, C. (1995). Multiple essential functions of neuregulin in development. *Nature* *378*, 386–390.
  44. Fukuda, R., Aharonov, A., Ong, Y.T., Stone, O.A., El-Brolosy, M., Maischein, H.M., Potente, M., Tzahor, E., and Stainier, D. Y. (2019). Metabolic modulation regulates cardiac wall morphogenesis in zebrafish. *Elife* *8*, e50161.
  45. Chan, R., Hardy, W.R., Laing, M.A., Hardy, S.E., and Muller, W.J. (2002). The catalytic activity of the ErbB-2 receptor tyrosine kinase is essential for embryonic development. *Mol. Cell Biol.* *22*, 1073–1078.
  46. Grego-Bessa, J., Luna-Zurita, L., del Monte, G., Bolós, V., Melgar, P., Arandilla, A., Garratt, A.N., Zang, H., Mukoyama, Y. S., Chen, H., et al. (2007). Notch signaling is essential for ventricular chamber development. *Dev. Cell* *12*, 415–429.
  47. Seidman, A., Hudis, C., Pierri, M.K., Shak, S., Paton, V., Ashby, M., Murphy, M., Stewart, S.J., and Keefe, D. (2002). Cardiac dysfunction in the trastuzumab clinical trials experience. *J. Clin. Oncol.* *20*, 1215–1221.
  48. Olayioye, M.A., Neve, R.M., Lane, H.A., and Hynes, N.E. (2000). The ErbB signaling network: receptor heterodimerization in development and cancer. *EMBO J.* *19*, 3159–3167.
  49. Kilgore, H.R., and Raines, R.T. (2018). n→pi\* Interactions Modulate the Properties of Cysteine Residues and Disulfide Bonds in Proteins. *J. Am. Chem. Soc.* *140*, 17606–17611.
  50. Sevier, C.S., and Kaiser, C.A. (2002). Formation and transfer of disulphide bonds in living cells. *Nat. Rev. Mol. Cell Biol.* *3*, 836–847.
  51. Hwang, C., Sinskey, A.J., and Lodish, H.F. (1992). Oxidized redox state of glutathione in the endoplasmic reticulum. *Science* *257*, 1496–1502.

52. Riemer, J., Bulleid, N., and Herrmann, J.M. (2009). Disulfide formation in the ER and mitochondria: two solutions to a common process. *Science* *324*, 1284–1287.
53. Ding, Y., Liu, Z., Desai, S., Zhao, Y., Liu, H., Pannell, L.K., Yi, H., Wright, E.R., Owen, L.B., Dean-Colomb, W., et al. (2012). Receptor tyrosine kinase ErbB2 translocates into mitochondria and regulates cellular metabolism. *Nat. Commun.* *3*, 1271.
54. Yarden, Y., and Shilo, B.Z. (2007). SnapShot: EGFR signaling pathway. *Cell* *131*, 1018.
55. Yu, S., Hei, Y., and Liu, W. (2018). Upregulation of seladin-1 and nestin expression in bone marrow mesenchymal stem cell transplantation via the ERK1/2 and PI3K/Akt signaling pathways in an Alzheimer's disease model. *Oncol. Lett.* *15*, 7443–7449.
56. Mohamed, J.S., and Boriek, A.M. (2012). Loss of desmin triggers mechanosensitivity and up-regulation of Ankr1 expression through Akt-NF- $\kappa$ B signaling pathway in smooth muscle cells. *FASEB J.* *26*, 757–765.
57. Passer, D., van de Vrugt, A., Atmanli, A., and Domian, I.J. (2016). Atypical Protein Kinase C-Dependent Polarized Cell Division Is Required for Myocardial Trabeculation. *Cell Rep.* *14*, 1662–1672.
58. Luo, J., McMullen, J.R., Sobkiw, C.L., Zhang, L., Dorfman, A. L., Sherwood, M.C., Logsdon, M.N., Horner, J.W., DePinho, R.A., Izumo, S., and Cantley, L.C. (2005). Class IA phosphoinositide 3-kinase regulates heart size and physiological cardiac hypertrophy. *Mol. Cell Biol.* *25*, 9491–9502.
59. Lin, Z., Zhou, P., von Gise, A., Gu, F., Ma, Q., Chen, J., Guo, H., van Gorp, P.R.R., Wang, D.Z., and Pu, W.T. (2015). Pi3kcb links Hippo-YAP and PI3K-AKT signaling pathways to promote cardiomyocyte proliferation and survival. *Circ. Res.* *116*, 35–45.
60. Braz, J.C., Gregory, K., Pathak, A., Zhao, W., Sahin, B., Klevitsky, R., Kimball, T.F., Lorenz, J.N., Nairn, A.C., Liggett, S.B., et al. (2004). PKC- $\alpha$  regulates cardiac contractility and propensity toward heart failure. *Nat. Med.* *10*, 248–254.
61. Roberts, A.E., Araki, T., Swanson, K.D., Montgomery, K.T., Schiripo, T.A., Joshi, V.A., Li, L., Yassin, Y., Tamburino, A. M., Neel, B.G., and Kucherlapati, R.S. (2007). Germline gain-of-function mutations in *SOS1* cause Noonan syndrome. *Nat. Genet.* *39*, 70–74.
62. Tartaglia, M., and Gelb, B.D. (2005). Noonan syndrome and related disorders: genetics and pathogenesis. *Annu. Rev. Genom. Hum. Genet.* *6*, 45–68.
63. Martinelli, S., De Luca, A., Stellacci, E., Rossi, C., Checquolo, S., Lepri, F., Caputo, V., Silvano, M., Buscherini, F., Consoli, F., et al. (2010). Heterozygous germline mutations in the *CBL* tumor-suppressor gene cause a Noonan syndrome-like phenotype. *Am. J. Hum. Genet.* *87*, 250–257.
64. Birker, K., Ge, S., Kirkland, N.J., Theis, J.L., Marchant, J., Fogarty, Z.C., Missinato, M.A., Kalvakuri, S., Grossfeld, P., Engler, A.J., et al. (2023). Mitochondrial MICOS complex genes, implicated in hypoplastic left heart syndrome, maintain cardiac contractility and actomyosin integrity. *Elife* *12*, e83385.
65. Cao, Q., Shen, Y., Liu, X., Yu, X., Yuan, P., Wan, R., Liu, X., Peng, X., He, W., Pu, J., and Hong, K. (2017). Phenotype and Functional Analyses in a Transgenic Mouse Model of Left Ventricular Noncompaction Caused by a *DTNA* Mutation. *Int. Heart J.* *58*, 939–947.
66. Jin, S.C., Homsy, J., Zaidi, S., Lu, Q., Morton, S., DePalma, S. R., Zeng, X., Qi, H., Chang, W., Sierant, M.C., et al. (2017). Contribution of rare inherited and de novo variants in 2,871 congenital heart disease probands. *Nat. Genet.* *49*, 1593–1601.
67. Zhang, J., Lin, Y., Zhang, Y., Lan, Y., Lin, C., Moon, A.M., Schwartz, R.J., Martin, J.F., and Wang, F. (2008). *Frs2*alpha-deficiency in cardiac progenitors disrupts a subset of FGF signals required for outflow tract morphogenesis. *Development* *135*, 3611–3622.
68. Yalcin, H.C., Amindari, A., Butcher, J.T., Althani, A., and Yacoub, M. (2017). Heart function and hemodynamic analysis for zebrafish embryos. *Dev. Dyn.* *246*, 868–880.
69. Liu, J., and Stainier, D.Y.R. (2012). Zebrafish in the study of early cardiac development. *Circ. Res.* *110*, 870–874.
70. Liu, X., Yagi, H., Saeed, S., Bais, A.S., Gabriel, G.C., Chen, Z., Peterson, K.A., Li, Y., Schwartz, M.C., Reynolds, W.T., et al. (2017). The complex genetics of hypoplastic left heart syndrome. *Nat. Genet.* *49*, 1152–1159.
71. Huang, M., Akerberg, A.A., Zhang, X., Yoon, H., Joshi, S., Hallinan, C., Nguyen, C., Pu, W.T., Haigis, M.C., Burns, C.G., and Burns, C.E. (2022). Intrinsic myocardial defects underlie an *Rbfox*-deficient zebrafish model of hypoplastic left heart syndrome. *Nat. Commun.* *13*, 5877.
72. Yang, C., Xu, Y., Yu, M., Lee, D., Alharti, S., Hellen, N., Ahmad Shaik, N., Banaganapalli, B., Sheikh Ali Mohamoud, H., Elango, R., et al. (2017). Induced pluripotent stem cell modelling of HLHS underlines the contribution of dysfunctional NOTCH signalling to impaired cardiogenesis. *Hum. Mol. Genet.* *26*, 3031–3045.
73. Jiang, Y., Habibollah, S., Tilgner, K., Collin, J., Barta, T., Al-Aama, J.Y., Tesarov, L., Hussain, R., Trafford, A.W., Kirkwood, G., et al. (2014). An induced pluripotent stem cell model of hypoplastic left heart syndrome (HLHS) reveals multiple expression and functional differences in HLHS-derived cardiac myocytes. *Stem Cells Transl. Med.* *3*, 416–423.
74. Tomita-Mitchell, A., Stamm, K.D., Mahnke, D.K., Kim, M.S., Hidestrand, P.M., Liang, H.L., Goetsch, M.A., Hidestrand, M., Simpson, P., Pelech, A.N., et al. (2016). Impact of *MYH6* variants in hypoplastic left heart syndrome. *Physiol. Genom.* *48*, 912–921.
75. Paige, S.L., Galdos, F.X., Lee, S., Chin, E.T., Ranjbarvaziri, S., Feyen, D.A.M., Darsha, A.K., Xu, S., Ryan, J.A., Beck, A.L., et al. (2020). Patient-Specific Induced Pluripotent Stem Cells Implicate Intrinsic Impaired Contractility in Hypoplastic Left Heart Syndrome. *Circulation* *142*, 1605–1608.
76. Jordan, E., Peterson, L., Ai, T., Asatryan, B., Bronicki, L., Brown, E., Celeghein, R., Edwards, M., Fan, J., Ingles, J., et al. (2021). Evidence-Based Assessment of Genes in Dilated Cardiomyopathy. *Circulation* *144*, 7–19.
77. Kaski, J.P., Syrris, P., Burch, M., Tomé-Esteban, M.T., Fenton, M., Christiansen, M., Andersen, P.S., Sebire, N., Ashworth, M., Deanfield, J.E., et al. (2008). Idiopathic restrictive cardiomyopathy in children is caused by mutations in cardiac sarcomere protein genes. *Heart* *94*, 1478–1484.
78. Tadros, H.J., Life, C.S., Garcia, G., Pirozzi, E., Jones, E.G., Datta, S., Parvatiyar, M.S., Chase, P.B., Allen, H.D., Kim, J.J., et al. (2020). Meta-analysis of cardiomyopathy-associated variants in troponin genes identifies loci and intragenic hot spots that are associated with worse clinical outcomes. *J. Mol. Cell. Cardiol.* *142*, 118–125.
79. Miao, Y., Tian, L., Martin, M., Paige, S.L., Galdos, F.X., Li, J., Klein, A., Zhang, H., Ma, N., Wei, Y., et al. (2020). Intrinsic

- Endocardial Defects Contribute to Hypoplastic Left Heart Syndrome. *Cell Stem Cell* 27, 574–589.e8.
80. Aghajanian, H., Cho, Y.K., Manderfield, L.J., Herling, M.R., Gupta, M., Ho, V.C., Li, L., Degenhardt, K., Aharonov, A., Tzahor, E., and Epstein, J.A. (2016). Coronary vasculature patterning requires a novel endothelial ErbB2 holoreceptor. *Nat. Commun.* 7, 12038.
  81. Elliott, D.A., Kirk, E.P., Yeoh, T., Chandar, S., McKenzie, F., Taylor, P., Grossfeld, P., Fatkin, D., Jones, O., Hayes, P., et al. (2003). Cardiac homeobox gene NKX2-5 mutations and congenital heart disease: associations with atrial septal defect and hypoplastic left heart syndrome. *J. Am. Coll. Cardiol.* 41, 2072–2076.
  82. Chen, H., Shi, S., Acosta, L., Li, W., Lu, J., Bao, S., Chen, Z., Yang, Z., Schneider, M.D., Chien, K.R., et al. (2004). BMP10 is essential for maintaining cardiac growth during murine cardiogenesis. *Development* 131, 2219–2231.
  83. Pirinccioglu, A.G., Alyan, O., Kizil, G., Kangin, M., and Beyazit, N. (2012). Evaluation of oxidative stress in children with congenital heart defects. *Pediatr. Int.* 54, 94–98.
  84. Xu, X., Jin, K., Bais, A.S., Zhu, W., Yagi, H., Feinstein, T.N., Nguyen, P.K., Criscione, J.D., Liu, X., Beutner, G., et al. (2022). Uncompensated mitochondrial oxidative stress underlies heart failure in an iPSC-derived model of congenital heart disease. *Cell Stem Cell* 29, 840–855.e7.
  85. Engineer, A., Saiyin, T., Greco, E.R., and Feng, Q. (2019). Say NO to ROS: Their Roles in Embryonic Heart Development and Pathogenesis of Congenital Heart Defects in Maternal Diabetes. *Antioxidants* 8, 436.
  86. Sharma, S., Bhattarai, S., Ara, H., Sun, G., St Clair, D.K., Bhuiyan, M.S., Kevil, C., Watts, M.N., Dominic, P., Shimizu, T., et al. (2020). SOD2 deficiency in cardiomyocytes defines defective mitochondrial bioenergetics as a cause of lethal dilated cardiomyopathy. *Redox Biol.* 37, 101740.
  87. Kundumani-Sridharan, V., Subramani, J., Owens, C., and Das, K.C. (2021). Nrg1beta Released in Remote Ischemic Preconditioning Improves Myocardial Perfusion and Decreases Ischemia/Reperfusion Injury via ErbB2-Mediated Rescue of Endothelial Nitric Oxide Synthase and Abrogation of Trx2 Autophagy. *Arterioscler. Thromb. Vasc. Biol.* 41, 2293–2314.
  88. Lee, T.C., Zhao, Y.D., Courtman, D.W., and Stewart, D.J. (2000). Abnormal aortic valve development in mice lacking endothelial nitric oxide synthase. *Circulation* 101, 2345–2348.
  89. Aaronson, R.M., Graven, K.K., Tucci, M., McDonald, R.J., and Farber, H.W. (1995). Non-neuronal enolase is an endothelial hypoxic stress protein. *J. Biol. Chem.* 270, 27752–27757.
  90. Mizukami, Y., Iwamatsu, A., Aki, T., Kimura, M., Nakamura, K., Nao, T., Okusa, T., Matsuzaki, M., Yoshida, K.I., and Kobayashi, S. (2004). ERK1/2 regulates intracellular ATP levels through alpha-enolase expression in cardiomyocytes exposed to ischemic hypoxia and reoxygenation. *J. Biol. Chem.* 279, 50120–50131.
  91. Sanchez-Castro, M., Eldjouzi, H., Charpentier, E., Busson, P. F., Hauet, Q., Lindenbaum, P., Delasalle-Guyomarch, B., Baudry, A., Pichon, O., Pascal, C., et al. (2016). Search for Rare Copy-Number Variants in Congenital Heart Defects Identifies Novel Candidate Genes and a Potential Role for FOXC1 in Patients With Coarctation of the Aorta. *Circ. Cardiovasc. Genet.* 9, 86–94.
  92. Crone, S.A., Zhao, Y.Y., Fan, L., Gu, Y., Minamisawa, S., Liu, Y., Peterson, K.L., Chen, J., Kahn, R., Condorelli, G., et al. (2002). ErbB2 is essential in the prevention of dilated cardiomyopathy. *Nat. Med.* 8, 459–465.